

# Geophysical Research Letters



# RESEARCH LETTER

10.1029/2025GL116260

#### **Key Points:**

- Quasi-stationary waves respond differently to climate warming across wavenumbers under a medium-to-high emissions scenario
- High-amplitude Waves 3 and 7 are projected to occur more frequently, while Waves 4–6 may decline or remain unchanged
- More frequent high-amplitude Waves 3 and 7 are expected to increase concurrent humid-heat extremes in specific regions

#### **Supporting Information:**

Supporting Information may be found in the online version of this article.

#### Correspondence to:

J. Yuan, jcyuan@fudan.edu.cn

#### Citation:

Lin, Q., Yuan, J., Ting, M., & Zhang, R. (2025). Linking high-amplitude quasi-stationary waves with concurrent humid-heat extremes in a warming world. *Geophysical Research Letters*, 52, e2025GL116260. https://doi.org/10.1029/2025GL116260

Received 7 APR 2025 Accepted 9 JUL 2025

# **Author Contributions:**

Conceptualization: Jiacan Yuan Formal analysis: Qiyan Lin, Jiacan Yuan Funding acquisition: Jiacan Yuan, Renhe Zhang

Supervision: Jiacan Yuan Visualization: Qiyan Lin Writing – original draft: Qiyan Lin,

writing – original draft: Qiyan Lin

Jiacan Yuan

**Writing – review & editing:** Qiyan Lin, Jiacan Yuan, Mingfang Ting, Renhe Zhang

# © 2025. The Author(s).

This is an open access article under the terms of the Creative Commons
Attribution-NonCommercial-NoDerivs
License, which permits use and
distribution in any medium, provided the original work is properly cited, the use is non-commercial and no modifications or adaptations are made.

# **Linking High-Amplitude Quasi-Stationary Waves With Concurrent Humid-Heat Extremes in a Warming World**

Qiyan Lin<sup>1</sup>, Jiacan Yuan<sup>1</sup>, Mingfang Ting<sup>2</sup>, and Renhe Zhang<sup>1</sup>

<sup>1</sup>Department of Atmospheric and Oceanic Sciences & Institute of Atmospheric Sciences & Shanghai Key Laboratory of Ocean-land-atmosphere Boundary Dynamics and Climate Change, Fudan University, Shanghai, China, <sup>2</sup>Columbia Climate School, Columbia University, New York, NY, USA

**Abstract** Humid-heat extremes pose serious risks to human health. When occurring simultaneously across different regions, they can lead to widespread exposure and substantial economic loss. Previous studies have linked concurrent humid-heat extremes in the Northern Hemisphere midlatitudes to high-amplitude quasistationary waves (QSWs). However, how these waves respond to climate warming remains unclear, limiting our ability to assess future risks quantitatively. Using a single model initial-condition large ensemble, we find that the climatological-mean amplitude of wavenumbers 3 and 7 QSWs increases in late summer as the climate warms, along with more frequent high-amplitude Wave-3 and Wave-7 events. These changes are associated with increased regional frequencies of humid-heat extremes, particularly in regions with strong historical connections between humid-heat extremes and high-amplitude QSWs. Our findings help identify regions characterized by high-impact concurrent humid-heat extremes and improve understanding of spatially heterogeneous changes in humid-heat extremes in a warming climate.

Plain Language Summary Humidity can greatly amplify the impacts of high temperature. Often referred to as the "silent killer," humid-heat extremes pose serious threat to human health and labor productivity, with elevated consequences when co-occurring at multiple locations. Projecting these concurrent events and understanding the mechanisms behind their changes are essential for improving heat risk management at the local level. Here, we identify a potential mechanism linking climate warming to future changes in concurrent humid-heat extremes from the perspective of quasi-stationary waves. Our findings highlight high-risk regions where increases in these extremes are linked to projected changes in specific wavenumber quasi-stationary waves under climate warming.

## 1. Introduction

In recent decades, the significant socioeconomic impacts of concurrent weather extremes (i.e., events taking place in multiple locations simultaneously) have received increased attention from both the scientific community and the public (Ouyang et al., 2023; Zscheischler et al., 2020). For example, the summer of 2022 saw record-breaking and long-lasting high-temperature extremes across much of the Northern Hemisphere (NH) (Lu et al., 2022), affecting a large population across China (about 360 million people were exposed to temperatures above 40°C) (Witze, 2022), Europe (at least 15,000 heat-related deaths) (Kluge, 2022) and the United States (over 100 million people experienced excessive heat) (Cappucci & Samenow, 2022). Persistent high-temperature extremes again impacted multiple NH continents concurrently in the summer of 2023 (Perkins-Kirkpatrick et al., 2024; Yin et al., 2025). Compared to high-temperature extremes alone, humid-heat extremes, combining the effects of both high temperature and humidity, pose even greater risk to human health (Mora et al., 2017; Wehner et al., 2017). This is because the primary way of heat dissipation for the human body in hot weather is evaporative cooling through sweating, the efficiency of which is reduced under a high-humidity environment (Buzan & Huber, 2020). As the global mean surface temperature rises, humid-heat extremes are projected to increase in frequency, intensity as well as geographic extent, with notable regional differences (Li et al., 2020; Russo et al., 2017). However, the mechanisms linking climate warming to future changes in concurrent humid-heat extremes remain poorly understood.

Quasi-stationary waves (QSWs) are atmospheric Rossby waves that typically persist for 2 weeks to a month (Stendel et al., 2021; Wills et al., 2019). A growing number of studies have indicated that concurrent extreme events at the hemispheric scale can be driven by circumglobal wave trains, especially QSWs with enhanced

LIN ET AL.

amplitudes (Coumou et al., 2014; Wang et al., 2023; Xu et al., 2021; Yuan et al., 2015). It has been shown that high-amplitude QSWs of selected wavenumbers favor the simultaneous occurrence of humid-heat extremes at different locations of the NH midlatitudes by modifying some physical processes, such as temperature advection and moisture transport (Lin & Yuan, 2022). Thus, how QSWs may change as a consequence of climate warming can have crucial impacts on future changes of concurrent humid-heat extremes over the NH midlatitudes. Recent studies on how QSWs are intensified in the current climate have led to several hypotheses: (a) Arctic amplification may lead to slower-propagating, larger-amplitude Rossby waves (Cohen et al., 2014; Francis & Vavrus, 2012); (b) quasi-resonance between free waves along the waveguide and forced waves from orography or diabatic heating may amplify the quasi-stationary components of waves with zonal wavenumbers 6–8 (Coumou et al., 2014; Petoukhov et al., 2013); (c) traveling synoptic-scale Rossby waves repeatedly occur at the same geological locations may contribute to more wave persistence (Röthlisberger et al., 2019; Wirth et al., 2018); (d) a preference for specific phase positions of Rossby waves has been observed, potentially influencing wave behavior (Ding & Wang, 2005; Kornhuber et al., 2020). While some of these hypotheses remain debated (Blackport & Screen, 2020a, 2020b; White et al., 2021; Wirth & Polster, 2021), it is still important to address the question of how future QSWs may change under climate warming. Simulations from the Coupled Model Intercomparison Project 5 (CMIP5) indicate an increase in quasi-resonant amplification events (Mann et al., 2018) and a strengthening of the climatological-mean amplitude of subtropical stationary waves (Yuan et al., 2018) in response to increasing external radiative forcing. However, these future projections also show notable discrepancies among climate models, highlighting the importance of model selection when assessing future QSW changes. Notably, QSWs with different zonal wavenumbers influence extreme events in different regions (Screen & Simmonds, 2014), and may respond differently to climate warming (Chemke & Ming, 2020; X. Chen & Dai, 2022; Wills et al., 2019). Yet, limited attention has been paid to wavenumber-dependent responses of QSWs to warming and their impacts on future changes in concurrent humid-heat extremes.

This study aims to project changes in NH mid-latitude QSWs across the zonal wavenumber space under continued warming, and to further explore their impacts on future concurrent humid-heat extremes.

# 2. Data and Methods

# 2.1. CESM2-LE Simulations

We utilize simulations from Community Earth System Model version 2 Large Ensemble (CESM2-LE) provided by the National Center for Atmospheric Research (NCAR) (Danabasoglu et al., 2020; Rodgers et al., 2021). CESM2 performs well among CMIP6 models in representing NH stationary waves (Simpson et al., 2020). Its meridional wind patterns (Figure S1 in Supporting Information S1) and the statistical characteristics of high-amplitude QSW events during the historical period closely resemble those in the ERA5 reanalysis (Fei & White, 2023). Additionally, the single model initial-condition large ensemble (SMILE) simulations offer a large sample size, enabling more robust assessments of rare extreme events (Chen et al., 2021). Therefore, CESM2-LE not only helps reduce uncertainties related to model configurations, but also improves the robustness of extreme event estimates.

CESM2-LE is a 100-member ensemble with slightly different initial conditions but the same historical radiative forcing from 1850 to 2014 and SSP3-7.0 emissions scenario from 2015 to 2100 on a nominal 1-degree spatial resolution (Table S1 in Supporting Information S1). We analyze only the 40 micro-perturbation members that follow the standard CMIP6 biomass burning protocol for two main reasons: (a) to enable comparisons with other CMIP6 models, and (b) due to the data accessibility of the required variables for this study (Table S2 in Supporting Information S1). Given recent mitigation efforts following the 2015 Paris Agreement, SSP5-8.5 is now considered an unlikely worst-case scenario (Hausfather & Peters, 2020). In this context, SSP3-7.0—the second highest emissions scenario—is recommended, particularly given its relevance for impact assessments (Shiogama et al., 2023). We regard 1965–2014 as the historical period (labeled "HIST") and 2051–2100 as the future period (labeled "SSP370"), and differences between the two periods reflect the changes under climate warming. Here, we focus on late summer months referring to July and August when extreme humid-heat days peak in the NH midlatitudes (Rogers et al., 2021). Our results are not sensitive to the inclusion of June or September (Figure S2 in Supporting Information S1).

LIN ET AL. 2 of 9

## 2.2. Wave Amplitudes and Phases

We examine the amplitudes and phases of QSWs in the monthly mean upper-tropospheric circulation. Following Lin and Yuan (2022), we perform a Fourier decomposition of the 300-hPa meridional wind ( $V_{300}$ ) averaged over 30°N to 60°N to separate the different wave components as follows:

$$V = A\sin(k\lambda - \varphi),\tag{1}$$

where A is the wave amplitude (unit: m s<sup>-1</sup>), k is the zonal wavenumber,  $\lambda$  is the longitude (unit: radians), and  $\varphi$  is the wave phase (unit: radians). The zonal wavenumber indicates the number of complete wave cycles around a latitude circle, while the corresponding amplitude reflects the strength of that wavenumber. The phase represents the longitudinal position of the wave relative to the dateline.

A high-amplitude QSW month is defined as one in which the wave amplitude exceeds a threshold based on its historical distribution. To test the sensitivity of high-amplitude month frequency changes to different threshold levels, we use three amplitude thresholds: 1.0, 1.5, and 2.0 standard deviations (STD). We ultimately select the most extreme threshold (i.e., 2.0 STD) to ensure that the identified QSW events are sufficiently strong while still retaining a sample size large enough for meaningful statistical analysis (Johnson, 1999). The detailed counts of high-amplitude months for each threshold are listed in Table S3 in Supporting Information S1.

#### 2.3. Humid-Heat Extremes

Among the various metrics used to assess humid heat, the wet bulb globe temperature (WBGT) is an internationally recognized measure of heat stress, particularly for industrial and military guidelines (Budd, 2008; Dunne et al., 2013; Li et al., 2017; Willett & Sherwood, 2012). However, WBGT is not a standard output variable from climate models. In this study, we calculate a simplified version of WBGT (sWBGT), assuming no dependence on solar radiation and wind effects (Li et al., 2020):

$$sWBGT = 0.7 * WBT + 0.3 * TSA.$$
 (2)

Here, WBT is the 2-m wet-bulb temperature and TSA is the 2-m air temperature over land, both are available from CESM2-LE at a 3-hourly interval. We compute 8-times daily sWBGT and further convert them to daily and monthly sWBGT.

Since global warming can contribute to future changes in humid-heat extremes, we first remove the global warming signal from daily sWBGT at each grid point. This is done using linear regression between sWBGT and global surface air temperature (GSAT) over 1965–2100. GSAT is computed as the weighted average reference height temperature (TREFHT) over the global region. An extreme humid-heat day is then defined as a day when the daily maximum sWBGT exceeds the calendar-day's 90th percentile, calculated using a 5-day window during the historical period. This threshold is based on all samples from the 40 ensemble members. The total number of such extreme humid-heat days is referred to as sWBGTX90. To assess the influence of high-amplitude QSWs on extreme humid-heat frequency, we compute the fraction of the number of extreme humid-heat days occurring during high-amplitude months relative to all late-summer months, referred to as the "ratio of sWBGTX90." This metric also captures the geographically inhomogeneous impacts of high-amplitude waves on humid-heat extremes.

# 3. Results

# 3.1. Response of Quasi-Stationary Waves to Climate Warming

QSWs with different zonal wavenumbers exhibit distinct responses in their 50-year averaged wave amplitude under warming (Figure 1). We focus on zonal wavenumbers 3–7 (Waves 3–7), as their climatological-mean amplitudes are substantially larger than those of other wavenumbers (Figure S3 in Supporting Information S1). Compared to the historical period, all 40 ensemble members project an increase in the 50-year mean amplitude of Wave 3 (ranging from 7.0% to 26.5%) and Wave 7 (ranging from 5.0% to 28.5%) in the future. In contrast, the mean amplitude of Wave 4 and Wave 5 decreases in 39 and 30 out of 40 members, respectively. For

LIN ET AL. 3 of 9

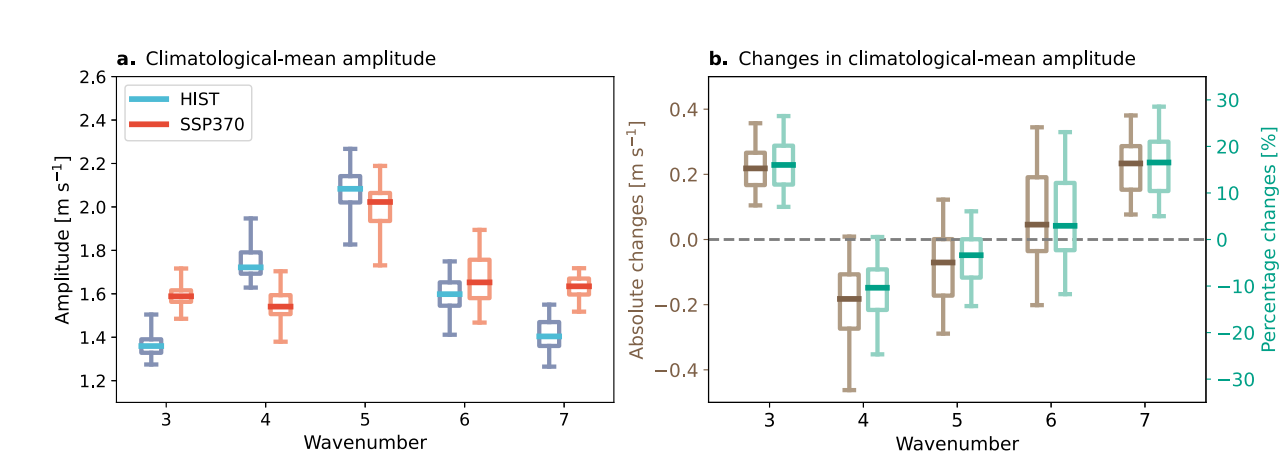


**Figure 1.** Comparison of climatological-mean wave amplitude between historical and future periods. (a) The 40-member distributions of 50-year averaged wave amplitude for the historical (blue) and future (red) periods. (b) The 40-member distributions of future changes in 50-year averaged wave amplitude are shown as absolute changes (i.e., SSP370-HIST, brown) and percentage changes (i.e., (SSP370-HIST)/HIST, green). Lines show median values, and boxes and caps provide the 25th–75th and 0th–100th percentile range, respectively.

Wave 6, approximately half of the ensemble members project an increase, while the other half indicate a decrease from the historical to future periods.

To determine the reasons behind changes in climatological-mean wave amplitude, we further compare monthly wave amplitudes between the historical and future periods across all members. This comparison reveals notable differences in the frequency of high-amplitude wave events (Table 1; Figure S4 in Supporting Information S1). Relative to the historical period, there is a significant increase in high-amplitude months for Wave 3 and Wave 7 during the future period for all three thresholds, indicating that the rise in high-amplitude Wave 3 and Wave 7

**Table 1**Comparison of Occurrence Frequency of High-Amplitude QSWs Between Historical and Future Periods

		HIST	SSP370	SSP370 - HIST	
1.0 STD	Wave 3	16.25%	27.35%	11.10%	**
	Wave 4	15.83%	8.98%	-6.85%	**
	Wave 5	16.80%	13.35%	-3.45%	**
	Wave 6	15.70%	17.90%	2.20%	**
	Wave 7	15.65%	24.73%	9.08%	**
1.5 STD	Wave 3	7.23%	14.80%	7.57%	**
	Wave 4	7.60%	3.38%	-4.22%	**
	Wave 5	7.85%	5.63%	-2.22%	**
	Wave 6	8.10%	9.00%	0.90%	
	Wave 7	7.53%	14.08%	6.55%	**
2.0 STD	Wave 3	2.90%	6.63%	3.73%	**
	Wave 4	3.23%	1.15%	-2.08%	**
	Wave 5	3.08%	1.55%	-1.53%	**
	Wave 6	3.98%	3.63%	-0.35%	
	Wave 7	3.38%	7.10%	3.72%	**

*Note.* Months of high-amplitude QSWs are respectively defined as those in which wave amplitude exceeds 1.0, 1.5, or 2.0 STDs of its historical distribution. Asterisks (\*\*) denote that occurrence frequency changes are statistically significant at the 99% confidence level based on the nonparametric bootstrap significance test.

frequencies is robust to the choice of threshold. In contrast, the frequency of high-amplitude months for Wave 4 and Wave 5 decreases slightly at all three thresholds. For Wave 6, high-amplitude months defined using the 1.0 STD threshold become more frequent, but no significant changes are seen at the 1.5 or 2.0 STD. These results suggest that changes in the 50-year averaged wave amplitude are closely linked to changes in the frequency of high-amplitude QSW months for each wavenumber under climate warming.

Given that high-amplitude Wave 3 (Liu et al., 2022; Screen & Simmonds, 2014) and Wave 7 (Kornhuber et al., 2019; Petoukhov et al., 2013) are shown to be associated with extreme events, we focus our analysis on these two wavenumbers, whose occurrence frequencies are projected to increase significantly in response to future warming. In both historical and future periods, the phase distributions of Wave 3 and Wave 7 during high-amplitude months (solid lines) show a highly symmetric single peak, and are sharper than those for all late-summer months (dashed lines) (Figures 2a and 2c). This suggests that high-amplitude Waves 3 and 7 tend to occur at preferred longitudes for their ridges and troughs. As a result, the composite uppertropospheric circulations during high-amplitude Wave-3 and Wave-7 months exhibit clear circumglobal wave patterns with the corresponding wavenumbers in both the historical and future periods (Figures 2b and 2d). Moreover, the phase distributions for the future period closely resemble those for the historical period, with little to no shift in the mean or peak positions (Figures 2a and 2c). The composite wave patterns in the future period largely overlap with those in the historical period (Figures 2b and 2d), indicating that the key regions influenced by high-amplitude QSWs during the historical period are expected to remain largely unchanged in location and will continue to be affected by high-amplitude QSWs in the future.

LIN ET AL. 4 of 9

1944/8007, 2025, 17, Downloaded from https://augupubs.onlinelibrary.wiley.com/doi/10.1029/2025GL116260, Wiley Online Library on [01/102025]. See the Terms and Conditions (https://onlinelibrary.wiley.com/terms-and-conditions) on Wiley Online Library for rules of use; OA articles are governed by the applicable Creative Commons Licensia

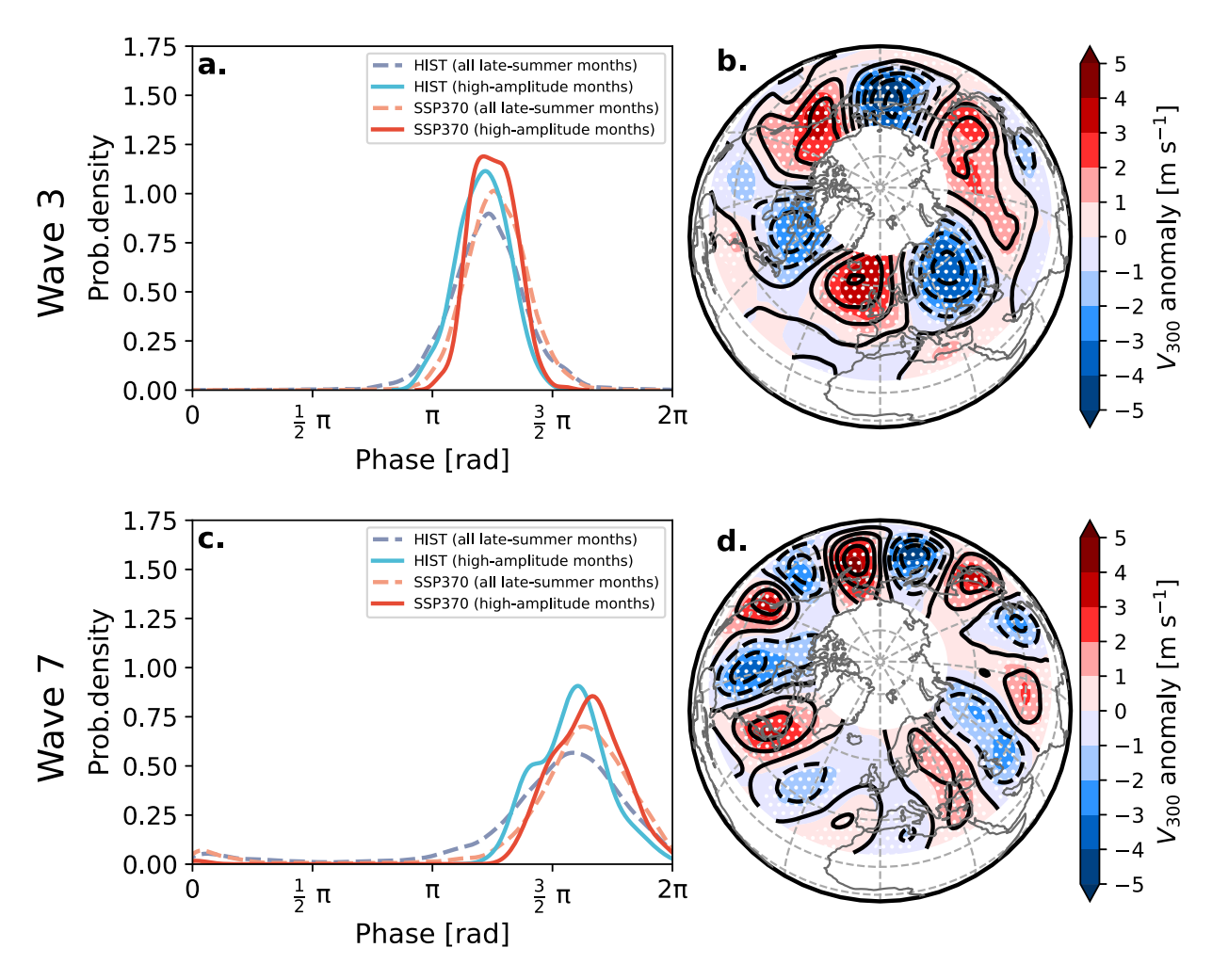


**Figure 2.** Comparison of phase distributions and upper-tropospheric wave patterns between historical and future periods. Probability densities of the phase positions for (a) Wave 3 and (c) Wave 7 during the historical (blue) and future (red) periods, with solid lines representing high-amplitude months and dashed lines representing all late-summer months. Composite  $V_{300}$  anomalies during months of high-amplitude (b) Wave 3 and (d) Wave 7 in the historical (shadings) and future (contours, contour interval =  $0.6 \text{ m s}^{-1}$ ) periods. White stipplings indicate the anomalies in the historical period are statistically significant at the 99% confidence level using a Monte Carlo test.

# 3.2. Projected Changes in Associated Humid-Heat Extremes

To determine whether CESM2-LE is a reliable tool for projecting changes in humid-heat extremes, we first examine the relationship between high-amplitude OSWs and humid-heat extremes during the historical period (Figures 3a-3d). During high-amplitude Wave-3 months, significantly positive sWBGT anomalies are found over north-central North America, western Europe and northeast Asia (Figure 3a). This pattern is consistent with previous studies that identified a similar zonal wavenumber-3 structure near 60°N in both upper-level circulation trends and surface warming (Liu et al., 2022). For Wave 7, sWBGT are significantly increased in Alaska, western North America, the Caspian Sea region as well as the Sichuan-Tibet region of China, with smaller increases in northeast Asia in high-amplitude months (Figure 3b). These regional warming patterns are consistent with earlier findings linking high temperatures in these regions to an intensified wavenumber-7 teleconnection (Kornhuber et al., 2019, 2020). Overall, the key regions of increased near-surface sWBGT correspond well with areas experiencing anomalous upper-tropospheric southerly flow or high-pressure system, characterized by southerly winds on the western flank and northerly winds on the eastern flank (Figures 2b and 2d). Such circulation regimes increase warm air advection, leading to significantly positive temperature anomalies (Figures S5a-S5d in Supporting Information S1), and simultaneously increase humidity through stronger moisture transport (Figures S5e– S5h in Supporting Information S1). The combined positive anomalies of temperature and humidity contribute to positive sWBGT anomalies in the key regions, where high-amplitude QSWs create persistent weather conditions

LIN ET AL. 5 of 9

1944/8007, 2025, 17, Downloaded from https://augupubs.onlinelibrary.wiley.com/doi/10.1029/2025GL116260, Wiley Online Library on [01/102025]. See the Terms and Conditions (https://onlinelibrary.wiley.com/terms-and-conditions) on Wiley Online Library for rules of use; OA articles are governed by the applicable Creative Commons Licens

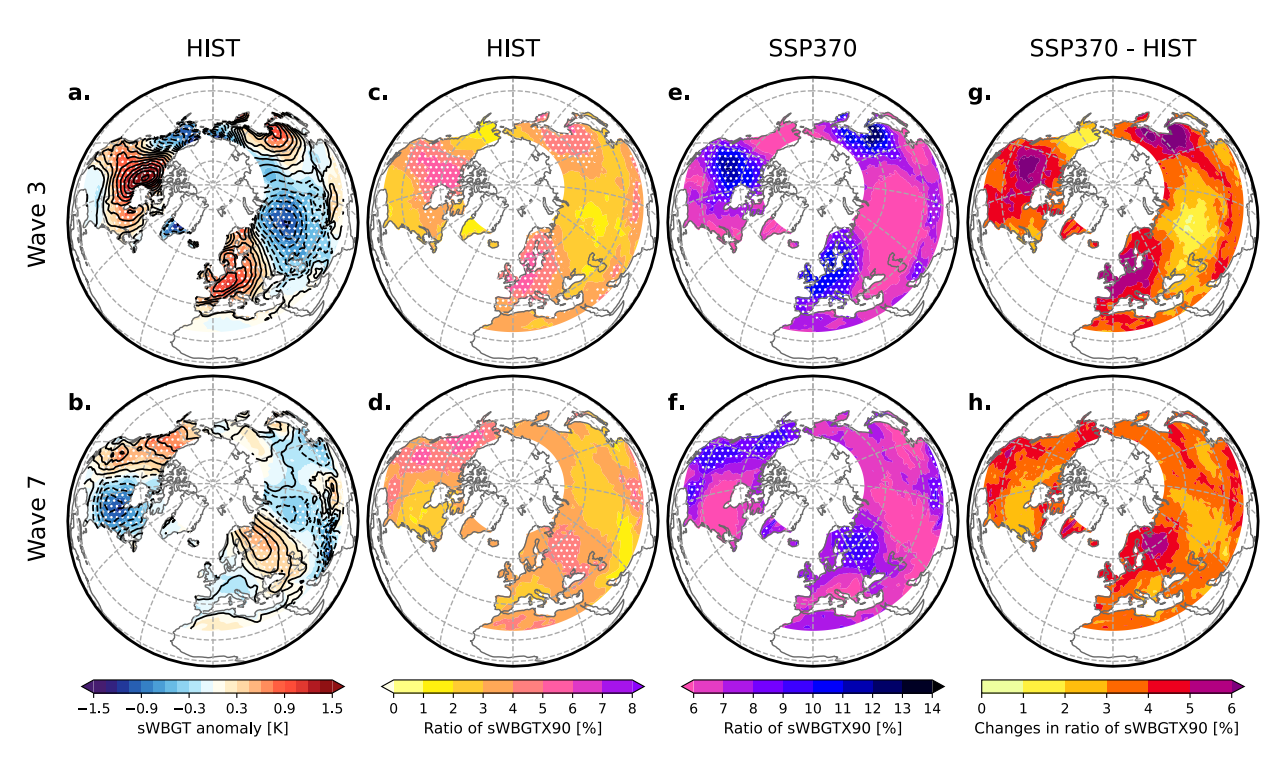


**Figure 3.** Comparison of humid-heat extremes associated with high-amplitude QSWs between historical and future periods. Composite sWBGT anomalies for high-amplitude (a) Wave 3 and (b) Wave 7 during the historical (shading) and future (contours, contour interval = 0.15 K) periods. The ratio of sWBGTX90 for high-amplitude (c, e) Wave 3 and (d and f) Wave 7 during the (c, d) historical and (e, f) future periods. Differences in the ratio of sWBGTX90 for high-amplitude (g) Wave 3 and (h) Wave 7 from the historical to future periods. Stipplings in (a–f) represent values statistically significant at the 99% confidence level using a Monte Carlo test.

that may fuel near-surface extreme events. During months of high-amplitude Wave 3 and Wave 7, the ratio of sWBGTX90 is indeed noticeably larger in the regions with elevated sWBGT than that in the other regions of the NH midlatitudes (Figures 3c and 3d). This indicates that the likelihood of humid-heat extremes over the specific regions identified above is higher during months characterized by high-amplitude Wave 3 and Wave 7. The key regions influenced by high-amplitude Wave 3 and Wave 7 are largely distinct, highlighting the need to analyze different wavenumber QSWs separately when assessing their impacts on extreme events.

In the future period, sWBGT is projected to increase over the above identified regions during months of highamplitude Wave 3 and Wave 7, relative to the climatological mean (contours in Figures 3a and 3b). These increases are accompanied by significantly positive anomalies in key variables, including temperature, temperature advection, specific humidity, and moisture flux (Figure S6 in Supporting Information S1). We further examine changes in humid-heat extremes associated with high-amplitude waves of both wavenumbers from the historical to future periods (Figures 3c-3h). The ratio of sWBGTX90 for high-amplitude Waves 3 and 7 in the future period depicts identical spatial patterns to that in the historical period. Their spatial correlation coefficients over land are 0.91 (p < 0.01) for Wave 3 and 0.87 (p < 0.01) for Wave 7. Associated with more frequent high-amplitude Waves 3 and 7, the ratio of sWBGTX90 increases over land in the future period relative to the historical period. However, this increase is spatially non-uniform across different regions. Specifically, the ratio of sWBGTX90 increases more sharply over north-central North America, western Europe and northeast Asia, caused by the occurrence frequency change in high-amplitude Wave 3. As for changes in the occurrence frequency of high-amplitude Wave 7, they lead to a notable magnification in the ratio of sWBGTX90 over Alaska, the continental United States, Europe, Western and North China as well as northeast Asia. These regions generally match the key regions where humid-heat extremes are connected to high-amplitude Wave 3 and Wave 7 in the historical period. In summary, as the climate warms, more frequent high-amplitude Wave 3 and Wave 7 are projected to substantially increase the frequency of humid-heat extremes in specific regions. These regions can be identified based on historical relationships between high-amplitude QSWs and humid-heat extremes.

LIN ET AL. 6 of 9

## 4. Conclusions and Discussions

The analyses of both reanalysis data (Lin & Yuan, 2022) and CESM2-LE simulations (Figures 3a–3d) consistently reveal strong relationships between high-amplitude QSWs and humid-heat extremes across the NH midlatitudes in the current climate. High-amplitude QSWs of specific wavenumbers provide favorable conditions for concurrent near-surface humid-heat extremes over particular regions. These regions typically coincide with areas experiencing southerly wind anomalies or high-pressure anomalies, corresponding to ridges of QSWs. In response to anthropogenic climate change, the frequency of high-amplitude Wave 3 and Wave 7 defined at all three thresholds (i.e., 1.0, 1.5, and 2.0 STDs) are expected to increase significantly based on our analysis of CESM2-LE simulations (Table 1), which aligns with the projected increase of their climatological-mean wave amplitudes (Figure 1). Additionally, the preferred phase positions and composite wave patterns of high-amplitude Wave 3 and Wave 7 remain largely unchanged in a warmer climate (Figure 2), suggesting that the regions historically influenced by these waves will continue to be affected in the future.

The projected changes in QSW behavior have important implications for future concurrent humid-heat extremes. We find that the increased frequency of high-amplitude Waves 3 and 7 will lead to a greater number of extreme humid-heat days in specific regions (Figures 3c-3h). Notably, these high-impact locations can be identified based on their historical connections to high-amplitude QSWs. As a result, simultaneous increases in humid-heat extremes across these areas could lead to widespread socioeconomic and ecological impacts on a global scale.

Quasi-stationary wave simulations can vary across climate models (Gong et al., 2018; Sun & Wang, 2023; Wills et al., 2019; Yuan et al., 2018). To assess model dependence in future projections, we examine changes in Wave 3 and Wave 7 using four additional large ensembles (Figure S7 in Supporting Information S1). The climatological-mean amplitude of Wave 3 is consistently projected to increase across nearly all members of these models, indicating a robust response to future warming. In contrast, projections of Wave 7 show greater variability across models. Most members project a decrease in Wave-7 amplitude, with only a small subset from CanESM5, EC-Earth3 and MPI-ESM1-2-LR showing an increase. This highlights model uncertainty in simulating the response of Wave 7 to warming, which may arise from differences in how models represent wave forcing changes, such as diabatic heating (Park & Lee, 2021). Stationary wave changes depend on several factors, including the zonal-mean basic state, zonally asymmetric forcings (e.g., topography, diabatic heating, transient eddies), and nonlinear interactions (Held et al., 2002; Ting, 1994; Ting & Yu, 1998). The projected amplification of Wave 3 and Wave 7 may result from changes in some of these factors under climate warming, which could create conditions more favorable for intensified wave amplitude. However, further research is needed to better understand the mechanisms behind these changes and to improve confidence in projections of QSW behavior in a warmer climate.

There are several limitations of this study. A common approach in previous research for identifying QSWs involves analyzing time-averaged fields, such as the monthly means used in this study, to filter out transient Rossby wave components and retain the quasi-stationary signals (Coumou et al., 2017; Petoukhov et al., 2013; Wolf et al., 2018). However, it is important to note that transient Rossby waves that repeatedly occur at a fixed longitudes within a month can also leave an imprint on monthly mean patterns (Ali et al., 2021; Röthlisberger et al., 2019). Therefore, while monthly averaged wave patterns effectively capture quasi-stationary Rossby waves that persist in the same location, they may also reflect the effects of recurrent transient waves anchored at specific longitudes. In this study, we do not explicitly separate wave signals by timescale; instead, we use monthly means to identify statistical patterns in which troughs and ridges consistently form in the same geographical regions. These persistent patterns are particularly relevant for driving humid-heat extremes, as they create persistent weather conditions that amplify near-surface impacts. Additionally, caution is warranted when interpreting metrics derived from Fourier analysis. High-amplitude QSWs identified through this method can result from strong regional features and do not necessarily represent hemispheric-scale patterns as illustrated by the composite circumglobal wave structures in Figures 2b and 2d.

In summary, our study highlights the projected increase in high-amplitude waves with multiple zonal wavenumbers under climate warming and their role in driving concurrent humid-heat extremes in affected regions. These findings offer critical insights into identifying key regions vulnerable to concurrent humid-heat extremes, shaped by the persistent influence of specific wave patterns. Populations in these hotspot regions are likely to face an increasing frequency of humid-heat extremes, underscoring the urgent need for region-specific adaptation strategies to mitigate the escalating societal and environmental risks posed by such events.

LIN ET AL. 7 of 9

19448007, 2025, 17, Downloaded from https://agupubs.onlinelibrary.wiley.com/doi/10.1029/2025GL116260,

# **Data Availability Statement**

CESM2-LE is accessed at <a href="https://www.cesm.ucar.edu/community-projects/lens2/data-sets">https://www.cesm.ucar.edu/community-projects/lens2/data-sets</a>. Large ensembles from CMIP6 models are available from Earth System Grid Federation (ESGF) at <a href="https://aims2.llnl.gov/search/cmip6/">https://aims2.llnl.gov/search/cmip6/</a>. ERA5 reanalysis can be downloaded through the Copernicus Climate Data Store (Hersbach et al., 2023). Derived data supporting this study are available from Zenodo repository via Lin (2025).

#### Acknowledgments

This study is supported by the National Natural Science Foundation of China (Grants 42288101 and 42175066). M.T. is supported by the National Science Foundation Grant AGS-1934358.

#### References

- Ali, S. M., Martius, O., & Röthlisberger, M. (2021). Recurrent Rossby wave packets modulate the persistence of dry and wet spells across the globe. *Geophysical Research Letters*, 48(5), e2020GL091452. https://doi.org/10.1029/2020GL091452
- Blackport, R., & Screen, J. A. (2020a). Insignificant effect of Arctic amplification on the amplitude of midlatitude atmospheric waves. *Science Advances*, 6(8), eaay2880. https://doi.org/10.1126/sciadv.aay2880
- Blackport, R., & Screen, J. A. (2020b). Weakened evidence for mid-latitude impacts of Arctic warming. *Nature Climate Change*, 10(12), 1065–1066. https://doi.org/10.1038/s41558-020-00954-y
- Budd, G. M. (2008). Wet-bulb globe temperature (WBGT)—Its history and its limitations. *Journal of Science and Medicine in Sport*, 11(1), 20–32. https://doi.org/10.1016/j.jsams.2007.07.003
- Buzan, J. R., & Huber, M. (2020). Moist heat stress on a hotter Earth. Annual Review of Earth and Planetary Sciences, 48(1), 623–655. https://doi.org/10.1146/annurey-earth-053018-060100
- Cappucci, M., & Samenow, J. (2022). Brutal heat from Phoenix to Boston triggers alerts for 100 million. Washington Post. Retrieved from https://www.washingtonpost.com/climate-environment/2022/07/21/heatwave-heat-texas-us/
- Chemke, R., & Ming, Y. (2020). Large atmospheric waves will get stronger, while small waves will get weaker by the end of the 21st century.
- Geophysical Research Letters, 47(22), e2020GL090441. https://doi.org/10.1029/2020GL090441

  Chen, X., & Dai, A. (2022). Response of Meridional wind to greenhouse gas forcing, Arctic sea-ice loss, and Arctic amplification. Journal of
- Climate, 35(22), 7275–7297. https://doi.org/10.1175/JCLI-D-22-0023.1 Chen, Y., Liao, Z., Shi, Y., Tian, Y., & Zhai, P. (2021). Detectable increases in sequential flood-heatwave events across China during 1961–2018.
- Geophysical Research Letters, 48(6), e2021GL092549. https://doi.org/10.1029/2021GL092549

  Cohen, J., Screen, J. A., Furtado, J. C., Barlow, M., Whittleston, D., Coumou, D., et al. (2014). Recent Arctic amplification and extreme mid-
- latitude weather. Nature Geoscience, 7(9), 627–637. https://doi.org/10.1038/ngeo2234
- Coumou, D., Kornhuber, K., Lehmann, J., & Petoukhov, V. (2017). Weakened flow, persistent circulation, and prolonged weather extremes in boreal summer. In Climate Extremes (pp. 61–73). American Geophysical Union (AGU). https://doi.org/10.1002/9781119068020.ch4
- Coumou, D., Petoukhov, V., Rahmstorf, S., Petri, S., & Schellnhuber, H. J. (2014). Quasi-resonant circulation regimes and hemispheric synchronization of extreme weather in boreal summer. Proceedings of the National Academy of Sciences of the United State of America, 111(34), 12331–12336. https://doi.org/10.1073/pnas.1412797111
- Danabasoglu, G., Lamarque, J.-F., Bacmeister, J., Bailey, D. A., DuVivier, A. K., Edwards, J., et al. (2020). The Community Earth System Model Version 2 (CESM2). Journal of Advances in Modeling Earth Systems, 12(2), e2019MS001916. https://doi.org/10.1029/2019MS001916
- Ding, Q., & Wang, B. (2005). Circumglobal teleconnection in the Northern Hemisphere summer. *Journal of Climate*, 18(17), 3483–3505. https://doi.org/10.1175/JCLI3473.1
- Dunne, J. P., Stouffer, R. J., & John, J. G. (2013). Reductions in labour capacity from heat stress under climate warming. *Nature Climate Change*, 3(6), 563–566. https://doi.org/10.1038/nclimate1827
- Fei, C., & White, R. H. (2023). Large-amplitude quasi-stationary Rossby wave events in ERA5 and the CESM2: Features, precursors, and model biases in Northern Hemisphere winter. *Journal of the Atmospheric Sciences*, 80, 2075–2090. https://doi.org/10.1175/JAS-D-22-0042.1
- Francis, J. A., & Vavrus, S. J. (2012). Evidence linking Arctic amplification to extreme weather in mid-latitudes. *Geophysical Research Letters*, 39(6), L06801. https://doi.org/10.1029/2012GL051000
- Gong, H., Wang, L., Chen, W., Wu, R., Huang, G., & Nath, D. (2018). Diversity of the Pacific–Japan Pattern among CMIP5 Models: Role of SST anomalies and atmospheric mean flow. *Journal of Climate*. 31(17), 6857–6877. https://doi.org/10.1175/JCLI-D-17-0541.1
- Hausfather, Z., & Peters, G. P. (2020). Emissions—The "business as usual" story is misleading. *Nature*, 577(7792), 618–620. https://doi.org/10.1038/d41586-020-00177-3
- Held, I. M., Mingang, T., & Hailan, W. (2002). Northern winter stationary waves: Theory and modeling. *Journal of Climate*, 15(16), 2125–2144. https://doi.org/10.1175/1520-0442(2002)015<2125:NWSWTA>2.0.CO;2
- Hersbach, H., Bell, B., Berrisford, P., Biavati, G., Horányi, A., Muñoz Sabater, J., et al. (2023). ERA5 monthly averaged data on pressure levels from 1940 to present [Dataset]. Copernicus Climate Change Service (C3S) Climate Data Store (CDS). https://doi.org/10.24381/cds.6860a573 Johnson, D. H. (1999). The insignificance of statistical significance testing. Journal of Wildlife Management, 63(3), 763–772. https://doi.org/10.24381/cds.0rg/10.24381/cds.0rg/10.24381/cds.0rg/10.24381/cds.0rg/10.24381/cds.0rg/10.24381/cds.0rg/10.24381/cds.0rg/10.24381/cds.0rg/10.24381/cds.0rg/10.24381/cds.0rg/10.24381/cds.0rg/10.24381/cds.0rg/10.24381/cds.0rg/10.24381/cds.0rg/10.24381/cds.0rg/10.24381/cds.0rg/10.24381/cds.0rg/10.24381/cds.0rg/10.24381/cds.0rg/10.24381/cds.0rg/10.24381/cds.0rg/10.24381/cds.0rg/10.24381/cds.0rg/10.24381/cds.0rg/10.24381/cds.0rg/10.24381/cds.0rg/10.24381/cds.0rg/10.24381/cds.0rg/10.24381/cds.0rg/10.24381/cds.0rg/10.24381/cds.0rg/10.24381/cds.0rg/10.24381/cds.0rg/10.24381/cds.0rg/10.24381/cds.0rg/10.24381/cds.0rg/10.24381/cds.0rg/10.24381/cds.0rg/10.24381/cds.0rg/10.24381/cds.0rg/10.24381/cds.0rg/10.24381/cds.0rg/10.24381/cds.0rg/10.24381/cds.0rg/10.24381/cds.0rg/10.24381/cds.0rg/10.24381/cds.0rg/10.24381/cds.0rg/10.24381/cds.0rg/10.24381/cds.0rg/10.24381/cds.0rg/10.24381/cds.0rg/10.24381/cds.0rg/10.24381/cds.0rg/10.24381/cds.0rg/10.24381/cds.0rg/10.24381/cds.0rg/10.24381/cds.0rg/10.24381/cds.0rg/10.24381/cds.0rg/10.24381/cds.0rg/10.24381/cds.0rg/10.24381/cds.0rg/10.24381/cds.0rg/10.24381/cds.0rg/10.24381/cds.0rg/10.24381/cds.0rg/10.24381/cds.0rg/10.24381/cds.0rg/10.24381/cds.0rg/10.24381/cds.0rg/10.24381/cds.0rg/10.24381/cds.0rg/10.24381/cds.0rg/10.24381/cds.0rg/10.24381/cds.0rg/10.24381/cds.0rg/10.24381/cds.0rg/10.24381/cds.0rg/10.24381/cds.0rg/10.24381/cds.0rg/10.24381/cds.0rg/10.24381/cds.0rg/10.24381/cds.0rg/10.24381/cds.0rg/10.24381/cds.0rg/10.24381/cds.0rg/10.24381/cds.0rg/10.24381/cds.0rg/10.24381/cds.0rg/10.24381/cds.0rg/10.24381/cds.0rg/10.24381/cds.0rg/10.24381/cds.0rg/10.24381/cds.0rg/10.243
- Kluge, H. (2022). Statement—Climate change is already killing us, but strong action now can prevent more deaths. World Health Organization. Retrieved from https://www.who.int/europe/news/item/07-11-2022-statement---climate-change-is-already-killing-us--but-strong-action-now-can-prevent-more-deaths
- Kornhuber, K., Coumou, D., Vogel, E., Lesk, C., Donges, J. F., Lehmann, J., & Horton, R. M. (2020). Amplified Rossby waves enhance risk of concurrent heatwaves in major breadbasket regions. *Nature Climate Change*, 10(1), 48–53. https://doi.org/10.1038/s41558-019-0637-z
- Kornhuber, K., Osprey, S., Coumou, D., Petri, S., Petoukhov, V., Rahmstorf, S., & Gray, L. (2019). Extreme weather events in early summer 2018 connected by a recurrent hemispheric wave-7 pattern. Environmental Research Letters, 14(5), 054002. https://doi.org/10.1088/1748-9326/ab13bf
- Li, C., Zhang, X., Zwiers, F., Fang, Y., & Michalak, A. M. (2017). Recent very hot summers in northern hemispheric land areas measured by wet bulb globe temperature will be the norm within 20 years. *Earth's Future*, 5(12), 1203–1216. https://doi.org/10.1002/2017EF000639
- Li, D., Yuan, J., & Kopp, R. E. (2020). Escalating global exposure to compound heat-humidity extremes with warming. *Environmental Research Letters*, 15(6), 064003. https://doi.org/10.1088/1748-9326/ab7d04
- Lin, Q. (2025). Replication data and code for "linking high-amplitude quasi-stationary waves with concurrent humid-heat extremes in a warming world" [Dataset]. Zenodo. https://doi.org/10.5281/zenodo.15858376
- Lin, Q., & Yuan, J. (2022). Linkages between amplified quasi-stationary waves and humid heat extremes in Northern Hemisphere midlatitudes. Journal of Climate, 35(24), 4645–4658. https://doi.org/10.1175/JCLI-D-21-0952.1

LIN ET AL. 8 of 9

- Liu, Y., Sun, C., & Li, J. (2022). The boreal summer zonal wavenumber-3 trend pattern and its connection with surface enhanced warming. Journal of Climate, 35(2), 833–850. https://doi.org/10.1175/JCLI-D-21-0460.1
- Lu, R., Xu, K., Chen, R., Chen, W., Li, F., & Lv, C. (2022). Heat waves in summer 2022 and increasing concern regarding heat waves in general. Atmospheric and Oceanic Science Letters, 16(1), 100290. https://doi.org/10.1016/j.aosl.2022.100290
- Mann, M. E., Rahmstorf, S., Kornhuber, K., Steinman, B. A., Miller, S. K., Petri, S., & Coumou, D. (2018). Projected changes in persistent extreme summer weather events: The role of quasi-resonant amplification. *Science Advances*, 4(10), eaat3272. https://doi.org/10.1126/sciadv.aat3272
- Mora, C., Dousset, B., Caldwell, I. R., Powell, F. E., Geronimo, R. C., Bielecki, C. R., et al. (2017). Global risk of deadly heat. *Nature Climate Change*, 7(7), 501–506. https://doi.org/10.1038/nclimate3322
- Ouyang, H., Tang, X., Zhang, R., Baklanov, A., Brasseur, G., Kumar, R., et al. (2023). Resilience building and collaborative governance for climate change adaptation in response to a new state of more frequent and intense extreme weather events. *International Journal of Disaster Risk Science*, 14(1), 162–169. https://doi.org/10.1007/s13753-023-00467-0
- Park, M., & Lee, S. (2021). Is the stationary wave bias in CMIP5 simulations driven by latent heating biases? *Geophysical Research Letters*, 48(4), e2020GL091678. https://doi.org/10.1029/2020GL091678
- Perkins-Kirkpatrick, S., Barriopedro, D., Jha, R., Wang, L., Mondal, A., Libonati, R., & Kornhuber, K. (2024). Extreme terrestrial heat in 2023. Nature Reviews Earth & Environment, 5(4), 244–246. https://doi.org/10.1038/s43017-024-00536-y
- Petoukhov, V., Rahmstorf, S., Petri, S., & Schellnhuber, H. J. (2013). Quasiresonant amplification of planetary waves and recent Northern Hemisphere weather extremes. *Proceedings of the National Academy of Sciences of the United States of America*, 110(14), 5336–5341. https://doi.org/10.1073/pnas.1222000110
- Rodgers, K. B., Lee, S.-S., Rosenbloom, N., Timmermann, A., Danabasoglu, G., Deser, C., et al. (2021). Ubiquity of human-induced changes in climate variability. *Earth System Dynamics*, 12(4), 1393–1411. https://doi.org/10.5194/esd-12-1393-2021
- Rogers, C. D. W., Ting, M., Li, C., Kornhuber, K., Coffel, E. D., Horton, R. M., et al. (2021). Recent increases in exposure to extreme humid-heat events disproportionately affect populated regions. *Geophysical Research Letters*, 48(19), e2021GL094183. https://doi.org/10.1029/2021GL094183
- Röthlisberger, M., Frossard, L., Bosart, L. F., Keyser, D., & Martius, O. (2019). Recurrent synoptic-scale Rossby wave patterns and their effect on the persistence of cold and hot spells. *Journal of Climate*, 32(11), 3207–3226. https://doi.org/10.1175/JCLI-D-18-0664.1
- Russo, S., Sillmann, J., & Sterl, A. (2017). Humid heat waves at different warming levels. Scientific Reports, 7(1), 7477. https://doi.org/10.1038/
- Screen, J. A., & Simmonds, I. (2014). Amplified mid-latitude planetary waves favour particular regional weather extremes. *Nature Climate Change*, 4(8), 704–709. https://doi.org/10.1038/nclimate2271
- Shiogama, H., Fujimori, S., Hasegawa, T., Hayashi, M., Hirabayashi, Y., Ogura, T., et al. (2023). Important distinctiveness of SSP3–7.0 for use in impact assessments. *Nature Climate Change*, 13(12), 1276–1278. https://doi.org/10.1038/s41558-023-01883-2
- Simpson, I. R., Bacmeister, J., Neale, R. B., Hannay, C., Gettelman, A., Garcia, R. R., et al. (2020). An evaluation of the large-scale atmospheric circulation and its variability in CESM2 and other CMIP models. *Journal of Geophysical Research: Atmospheres*, 125(13), e2020JD032835. https://doi.org/10.1029/2020JD032835
- Stendel, M., Francis, J., White, R., Williams, P. D., & Woollings, T. (2021). The jet stream and climate change. In *Climate Change* (pp. 327–357). Elsevier. Retrieved from https://linkinghub.elsevier.com/retrieve/pii/B9780128215753000153
- Sun, W., & Wang, L. (2023). Diagnosing observed extratropical stationary wave changes in boreal winter. *Environmental Research Letters*, 18(11), 114014. https://doi.org/10.1088/1748-9326/acfb99
- Ting, M. (1994). Maintenance of northern summer stationary waves in a GCM. Journal of the Atmospheric Sciences, 51(22), 3286–3308. https://doi.org/10.1175/1520-0469(1994)051<3286:MONSSW>2.0.CO;2
- Ting, M., & Yu, L. (1998). Steady response to tropical heating in wavy linear and nonlinear Baroclinic models. *Journal of the Atmospheric Sciences*, 55(24), 3565–3582. https://doi.org/10.1175/1520-0469(1998)055<3565:SRTTHI>2.0.CO;2
- Wang, X., Zhang, R., Jin, D., & Zhang, Y. (2023). An intraseasonal dipole mode in summertime surface air temperature over Eurasia and its association with heat wave occurrence. *Journal of Climate*, 36(22), 7755–7770. https://doi.org/10.1175/JCLI-D-22-0761.1
- Wehner, M., Castillo, F., & Dáithí, S. (2017). The impact of moisture and temperature on human health in heat waves. Oxford Research Encyclopedia of Natural Hazard Science, 1–39. https://doi.org/10.1093/acrefore/9780199389407.013.58
- White, R. H., Kornhuber, K., Martius, O., & Wirth, V. (2021). From atmospheric waves to heatwaves: A waveguide perspective for understanding and predicting concurrent, persistent and extreme extratropical weather. *Bulletin of the American Meteorological Society*, 103(3), 1–35. https://doi.org/10.1175/BAMS-D-21-0170.1
- Willett, K. M., & Sherwood, S. (2012). Exceedance of heat index thresholds for 15 regions under a warming climate using the wet-bulb globe temperature. *International Journal of Climatology*, 32(2), 161–177. https://doi.org/10.1002/joc.2257
- Wills, R. C. J., White, R. H., & Levine, X. J. (2019). Northern Hemisphere stationary waves in a changing climate. *Current Climate Change Reports*, 5(4), 372–389. https://doi.org/10.1007/s40641-019-00147-6
- Wirth, V., & Polster, C. (2021). The problem of diagnosing jet waveguidability in the presence of large-amplitude eddies. *Journal of the Atmospheric Sciences*, 78(10), 3137–3151. https://doi.org/10.1175/JAS-D-20-0292.1
- Wirth, V., Riemer, M., Chang, E. K. M., & Martius, O. (2018). Rossby wave packets on the midlatitude waveguide—A review. *Monthly Weather Review*, 146(7), 1965–2001. https://doi.org/10.1175/MWR-D-16-0483.1
- Witze, A. (2022). Extreme heatwaves: Surprising lessons from the record warmth. Nature, 608(7923), 464–465. https://doi.org/10.1038/d41586-022-02114-y
- Wolf, G., Brayshaw, D. J., Klingaman, N. P., & Czaja, A. (2018). Quasi-stationary waves and their impact on European weather and extreme events. *Quarterly Journal of the Royal Meteorological Society*, 144(717), 2431–2448. https://doi.org/10.1002/qj.3310
- Xu, P., Wang, L., Vallis, G. K., Geen, R., Screen, J. A., Wu, P., et al. (2021). Amplified waveguide teleconnections along the polar front jet favor summer temperature extremes over Northern Eurasia. Geophysical Research Letters, 48(13), e2021GL093735. https://doi.org/10.1029/2021GL093735
- Yin, C., Ting, M., Kornhuber, K., Horton, R. M., Yang, Y., & Jiang, Y. (2025). CETD, a global compound events detection and visualisation toolbox and dataset. *Scientific Data*, 12(1), 356. https://doi.org/10.1038/s41597-025-04530-x
- Yuan, J., Li, W., & Deng, Y. (2015). Amplified subtropical stationary waves in boreal summer and their implications for regional water extremes. Environmental Research Letters, 10(10), 104009. https://doi.org/10.1088/1748-9326/10/104009
- Yuan, J., Li, W., Kopp, R. E., & Deng, Y. (2018). Response of subtropical stationary waves and hydrological extremes to climate warming in boreal summer. *Journal of Climate*, 31(24), 10165–10180. https://doi.org/10.1175/JCLI-D-17-0401.1
- Zscheischler, J., Martius, O., Westra, S., Bevacqua, E., Raymond, C., Horton, R. M., et al. (2020). A typology of compound weather and climate events. *Nature Reviews Earth & Environment*, 1(7), 333–347. https://doi.org/10.1038/s43017-020-0060-z

LIN ET AL. 9 of 9